
THE THERMODYNAMIC MODELING OF THE URANIUM-OXYGEN SYSTEM

Basuki A. Pudjanto

Pusbangtek Bahan Bakar Nuklir dan Daur Ulang – BATAN, Serpong
Centre for Development of Nuclear Fuel and Recycling Technology – BATAN,
Serpong

ABSTRACT

THE THERMODYNAMIC MODELING OF THE URANIUM-OXYGEN. The thermodynamic modeling of the uranium-oxygen (U–O) system, which is of first importance in the development of a nuclear thermodynamic database, has been performed. The thermodynamic properties of the phases present in the U–O system are described using the compound energy model with ionic constituents for the solids and an ionic two-sublattice model for the liquid. For the uranium dioxide, the structure is described using three sublattices, one for the cations U^{3+} , U^{4+} and U^{6+} , one for the normal site of oxygen ions, and one for the interstitial oxygen ions. Vacancies are included in both oxygen sublattices. In this first approach, the homogeneity ranges of the U_4O_{9-y} and U_3O_{8-y} compounds are not represented. Phase diagram and thermodynamic properties, then, have been calculated from the optimized Gibbs energy parameters, assuming that the system is in thermodynamic equilibrium, i.e. by finding the minimum for the total free energy of the system. The thermodynamic calculation is conducted through CALPHAD (Calculation Phase Diagram) approach, with the help from the Thermo-Calc code. The results obtained show that the consistency between the calculated results and the experimental data is quite satisfactory.

FREE TERMS: Nuclear fuel, Uranium oxide, Oxygen potential, Modeling, Thermodynamics

ABSTRAK

PEMODELAN TERMODINAMIK SISTEM URANIUM-OKSIGEN. *Pemodelan termodinamik sistem uranium-oksigen (U–O), yang penting sekali bagi pengembangan database termodinamik nuklir, telah dilakukan. Sifat-sifat termodinamik fasa-fasa yang ada dalam sistem U–O digambarkan menggunakan model ‘energi senyawa’ dengan model ‘konstituen ionik’ untuk fasa-fasa padat dan model ‘dua sub-lapis ionik’ untuk fasa cair. Sementara itu, struktur uranium dioksida digambarkan dengan model ‘tiga sub-lapis ionik’, satu sub-lapis untuk kation U^{3+} , U^{4+} dan U^{6+} , satu sub-lapis untuk kisi normal ion-ion oksigen dan satu sub-lapis lagi untuk interstisi ion-ion oksigen. Kekosongan-kekosongan dimasukkan ke dalam kedua sub-lapis oksigen. Pada kajian awal ini, rentang homogenitas senyawa U_4O_{9-y} dan U_3O_{8-y} tidak diberikan. Selanjutnya, diagram fasa dan sifat termodinamik dihitung dari optimasi parameter energi Gibbs, dengan asumsi bahwa sistem berada dalam kesetimbangan termodinamik, yaitu dengan mencari harga minimum dari energi bebas total sistem. Perhitungan dilakukan dengan pendekatan metode CALPHAD, dengan bantuan paket program Thermo-Calc. Hasil yang diperoleh menunjukkan konsistensi yang cukup memuaskan antara hasil perhitungan dan data eksperimen.*

KATA KUNCI: *Bahan bakar nuklir, Uranium oksida, Potensial oksigen, Pemodelan, Termodinamika*

I. INTRODUCTION

The thermodynamic modeling of the U–O system is of first importance in the development of a nuclear thermodynamic database. During a hypothetical severe accident, urania, submitted to high temperatures and various oxygen potentials, presents a wide non-stoichiometry range, i.e. the melting temperature of $\text{UO}_{2\pm x}$, related to oxygen potential, decreases in all cases^[1]. The fuel rods may melt and interact with other materials, leading to the core degradation. All materials of a nuclear plant may interact thermochemically: fuel (UO_2), zircaloy (Zr), steel structures (Fe, Cr, Ni), control rods (Ag, Cd, In) or boron carbide (B, C), fission products (Ba, La, Ru, Sr), concrete (Al_2O_3 , CaO, FeO, Fe_2O_3 , MgO, SiO_2), water and air (H, O)^[1]. That is why the thermodynamic modeling of the selected multicomponent system, based on the critical assessment of all the binary and the most important higher-order subsystems (metallic, oxide, metal-oxygen), becomes a useful tool to determine equilibrium conditions in such multicomponent and multiphase system. The critical assessment of the U–O binary system including the non-stoichiometry range of urania, then, is a major step to a correct thermodynamic modeling of multi-component systems for nuclear safety^[1], and the U–O binary system is the first of all.

In the present work, the thermodynamic properties of the phases present in the U–O system are described using the compound energy model with ionic constituents for the solids and an ionic two-sublattice model for the liquid. For the uranium dioxide, the structure is described using three sublattices, one for the cations U^{3+} , U^{4+} and U^{6+} , one for the normal site of oxygen ions, and one for the interstitial oxygen ions. Vacancies are included in both oxygen sublattices. In this first approach, the homogeneity ranges of the U_4O_{9-y} and U_3O_{8-y} compounds are not represented. Phase diagram and thermodynamic properties were calculated from the optimized Gibbs energy parameters, assuming that the system is in thermodynamic equilibrium, i.e. by finding the minimum for total free energy of the system. The thermodynamic calculation is conducted through CALPHAD (*Calculation Phase Diagram*) approach, with the help from the Thermo-Calc code^[2-4].

II. THEORY

The U–O binary system is certainly one of the most complex systems of the periodic table. The experimental information concerning phase diagram and thermodynamic properties is very numerous and their compilation has been undertaken for many years. Today, new experiments are available on the miscibility gap in the liquid state both in the U–O and O–U–Zr systems and the experimental methods for oxygen solubility measurements have been carefully re-analyzed to discard non-equilibrium measurements^[1,5-7]. Moreover, the set of experimental data has been completed: especially, very numerous oxygen potentials of $\text{UO}_{2\pm x}$ at various temperatures and phase diagram data in the hyperstoichiometric range ($\text{UO}_{2+x} + \text{U}_4\text{O}_{9-y}$) and ($\text{U}_4\text{O}_{9-y} + \text{U}_3\text{O}_{8-z}$) at low temperature have been taken into account; the heat capacity and heat content of stoichiometric compounds were also compiled in order to include second-order anomalies not previously described.

The uranium–oxygen system is characterized by a miscibility gap in the liquid state involving a metallic uranium rich liquid and an oxygen rich liquid, close to the UO_2 composition. The dioxide of uranium has a wide composition range at high temperature in which the thermodynamic properties depend on the O/U ratio. The numerous oxidation degrees of uranium lead to the existence of several complex oxides U_4O_9 , U_3O_8 and UO_3 . THERMODYNAMIC (France) and AEA Technology (UK) have developed thermodynamic

databases for the corium^[1] but the model for UO_{2-x} in these assessments was not satisfactory. In fact, the UO_{2+x} phase boundary at low temperature ($T < 1400$ K) and the corresponding change of the oxygen chemical potential are not well represented. Furthermore, THERMODYATA proposed two sets of thermodynamic parameters for the U–O system corresponding to two different descriptions of the miscibility gap^[1]. The critical analysis of the experimental data by LABROCHE and BAICHI^[5,6] allows GUÉNEAU et al.^[7] to propose a single description of the U–O system.

Chevalier and FISCHER^[1] have previously carried out a thermodynamic modeling of O–U–Zr system, from a critical assessment of all the available experimental information, equilibrium phase diagram and thermodynamic properties. Unfortunately, at that time, the experimental information provided by different sources was not consistent in some specific fields. The main identified incoherencies concerned the limit of solubility of oxygen in U or U–Zr alloys and the extension of the liquid miscibility gap in the U–O binary and O–U–Zr ternary systems. Owing to all the encountered experimental inconsistencies on the liquidus shape from 2073 K to very high temperatures (above 3000 K), two different sets of Gibbs energy parameters were proposed in CHEVALIER and FISCHER's previous work^[1] for the U–O and O–U–Zr ternary system. The first one corresponded to a small solubility of oxygen in U or U–Zr liquid alloys and a large miscibility gap, the second one to a larger solubility and a smaller miscibility gap. The two versions differed only on U–O and O–U–Zr excess interaction parameters, but did not succeed to reproduce simultaneously all the experimental points. From this analysis, it appeared obviously that future efforts should be made on the interpretation of the existing experiments in terms of thermodynamic equilibrium and that there was a lack of experimental information at high temperature.

All these points argue that a new critical assessment (phase diagram and thermodynamic properties) and thermodynamic modeling of the U–O binary system were quite necessary for building a high quality and reliable nuclear thermodynamic database.

III. GIBBS ENERGY MODELS

In the present study, the oxygen solubilities in the orthorhombic, tetragonal and bcc uranium phases are neglected. The U_4O_9 , U_3O_8 and UO_3 oxides are treated as single stoichiometric compounds. A future work will consist of the description of the composition ranges of U_4O_{9-y} and U_4O_{8-y} . The Gibbs energy functions for all the phases are referred to the enthalpy of the pure elements, i , in their stable state at room temperature 298.15 K and 1 bar (${}^0H_i^{\text{SER}}(298.15\text{ K})$).

3.1 Pure Elements

The Gibbs energy functions of the pure elements i at temperature T and in their state ϕ are given by:

$${}^0G_i^\phi(T) - {}^0H_i^{\text{SER}}(298.15\text{ K}) = a + bT = cT \ln T + \sum d_n T^n \quad (1)$$

where n is an integer (2, 3, -1, ...).

In the present work, DINSDALE's parameters are used for pure uranium^[8] and oxygen data are from SGTE 1997 Substance database^[9].

3.2 Stoichiometric Oxides

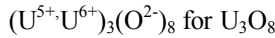
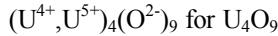
The stoichiometric oxides are described with two sublattices, one for the cations and one for the divalent oxygen ions.

The UO_3 oxide is described with the $(\text{U}^{6+})_1(\text{O}^{2-})_3$ two-sublattice model. The corresponding Gibbs energy function has the same form as in Eq. (1):

$${}^0G_i^{\phi}(T) - {}^0H_i^{\text{SER}}(298.15\text{ K}) = a + bT = cT \ln T + \sum d_n T^n \quad (2)$$

where n_i^{ϕ} is the number of atoms of the i th element in the oxide formula. The thermodynamic parameters have been taken from the SGTE 1997 Substance database^[9].

For both U_4O_9 and U_3O_8 oxides, a mixture of uranium charged species is assumed in the cation sublattice:



The free energy of the oxide with such a sublattice model $(\text{U}^{\square+}, \text{U}^{\square+})_p(\text{O}^{2-})_q$ in the state \square is expressed by:

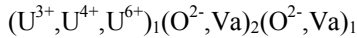
$$G^{\phi}(T) - p {}^0H_{\text{U}}^{\text{SER}}(298.15\text{K}) - q {}^0H_{\text{O}}^{\text{SER}}(298.15\text{K}) = y_{\text{U}^{\mu+}} {}^0G_{\text{U}^{\mu+}, \text{O}^{2-}} + y_{\text{U}^{\nu+}} {}^0G_{\text{U}^{\nu+}, \text{O}^{2-}} - pRT(y_{\text{U}^{\mu+}} \ln y_{\text{U}^{\mu+}} + y_{\text{U}^{\nu+}} \ln y_{\text{U}^{\nu+}}) \quad (3)$$

where y_i are the site fractions of the cations i in the first sublattice and the ${}^0G_{\text{U}^{\mu+}, \text{O}^{2-}}$ and ${}^0G_{\text{U}^{\nu+}, \text{O}^{2-}}$; Gibbs energy functions have the same description as in Eq. (2).

3.3 Non-stoichiometric Dioxide of Uranium $\text{UO}_{2\pm x}$

UO_2 adopts the fluorite structure which is typical of ionic compounds. An appreciable degree of covalence is expected in the material. UO_2 is known to behave as a semiconductor. The charge-transfer reaction $2\text{U}^{4+} = \text{U}^{5+} + \text{U}^{3+}$ is usually considered^[10]. This excitation process is thought to be responsible for the high temperature specific heat excess in the material. But the other charge states U^{2+} and U^{6+} may be also considered. In fact, it seems possible that charge-transfer processes lead to the generation of U^{2+} and U^{6+} as well as U^{3+} and U^{5+} at elevated temperatures. Therefore, in the present study, the uranium dioxide is described by using the compound energy model with ionic species.

The ideal structure of stoichiometric UO_2 is described with two sublattices, for U^{4+} and O^{2-} ions respectively. The hypostoichiometric side of UO_2 is modeled by introducing some oxygen vacancies in the normal oxygen sublattice. The charge balance is maintained by the presence of some U^{3+} ions in the uranium sublattice. The experimental studies of the hyperstoichiometric oxide show the presence of two types of interstitial oxygen atoms O' and O'' in positions that do not correspond to the classical interstitial sites of the fluorite structure^[11]. Therefore, a third sublattice for these interstitial oxygens is added to the two normal sublattices of the fluorite. To maintain the electro-neutrality, some U^{6+} cations are introduced in the uranium sublattice. In reality, as reported before, all the charges of uranium +2, +3, +4, +5 and +6 may be introduced in the cation sublattice. But this would considerably complicate the model by increasing the number of parameters to optimize. The structure of the $\text{UO}_{2\pm x}$ phase is then described by the following sublattice model:



The U^{6+} cation was chosen instead of U^{5+} as it allows to have a neutral end point (for the UO_3 composition). Moreover, by taking U^{5+} , the end composition would be equal to $UO_{2.5}$ that is very close to the real limit of UO_{2+x} . This could induce some troubles with the oxygen activities in this composition range of the dioxide. We have done a compromise by choosing U^{3+} to be consistent with the charge transfer reaction.

The number of sites of the interstitial oxygen sublattice is arbitrarily taken to be unity as neighboring sites are excluded due to electrostatic forces and size mismatch. The compound energy model gives the following expression for the Gibbs energy:

$$G^{\phi} - \sum_i n_i^{\phi} H_i^{SER} (298.15) \\ = y_{3+} y_O y'_O {}^0G_{3+:O} + y_{3+} y_O y'_V {}^0G_{3+:O:Va} + y_{3+} y_{Va} y'_O {}^0G_{3+:Va:O} + y_{3+} y_{Va} y'_V {}^0G_{3+:Va:Va} \\ + y_{4+} y_O y'_O {}^0G_{4+:O} + y_{4+} y_O y'_V {}^0G_{4+:O:Va} + y_{4+} y_{Va} y'_O {}^0G_{4+:Va:O} + y_{4+} y_{Va} y'_V {}^0G_{4+:Va:Va} \\ + y_{6+} y_O y'_O {}^0G_{6+:O} + y_{6+} y_O y'_V {}^0G_{6+:O:Va} + y_{6+} y_{Va} y'_O {}^0G_{6+:Va:O} + y_{6+} y_{Va} y'_V {}^0G_{6+:Va:Va} \\ + RT(y_{3+} \ln y_{3+} + y_{4+} \ln y_{4+} + y_{6+} \ln y_{6+}) + 2RT(y_O \ln y_O + y_{Va} \ln y_{Va}) \\ + RT(y_O \ln y_O + y_{Va} \ln y_{Va}) + G^E \quad (4)$$

where y_{3+} , y_{4+} and y_{6+} represent the fractions of uranium with different charges on the metallic sublattice, y_O and y_V are oxygen ions and vacancies respectively on the normal oxygen sublattice, y'_O and y'_V are oxygen ions and vacancies respectively on the interstitial oxygen sublattice. The 0G terms correspond to the Gibbs energies of the different compounds formed by considering one species in each sublattice. The model is shown as a prism in Figure 1. The triangular surfaces represent the change of uranium valency with constant occupancy of the other sublattices. Most of the corners correspond to unphysical compounds with a net charge. Among the compounds, the following ones are neutral:

4OV: $(U^{4+})_1(O^{2-})_2(VA)_1$, the ideal fluorite structure of UO_2

6OO: $(U^{6+})_1(O^{2-})_2(O^{2-})_1$, fully filled with the interstitial oxygen ions, of UO_3 composition

By combining oxygen ions and vacancies on the second and third sublattices, other neutral compounds can be generated:

$(U^{4+})_1(O^{2-}_{0.5}, VA_{0.25})_2(O^{2-})_1$ with composition UO_2

$(U^{3+})_1(O^{2-}_{0.75}, VA_{0.25})_2(VA)_1$ with composition $UO_{1.5}$

$(U^{3+})_1(O^{2-}_{0.25}, VA_{0.75})_2(O^{2-})_1$ with composition $UO_{1.5}$

By combination of these compounds, the area where the model for the dioxide of uranium is neutral can be determined (the two dashed surfaces with the ‘6OO’ common corner). In each domain, the composition of the phase ranges from $UO_{1.5}$ to UO_3 . The presence of these two domains shows that with the present model, the dioxide has several internal degrees of freedom, which can give some troubles in the optimization procedure.

The surface with the ‘4OV’ corner corresponding to the UO_2 ideal fluorite represents the correct domain of stability of the phase. It shows that the most important thermodynamic parameters to optimize are those of the ‘4OV’, ‘6OO’, ‘3OV’ and ‘3VV’ compounds. It was necessary to add an excess Gibbs energy term G^E to describe correctly the phase boundaries of UO_{2+x} . Some interaction terms L_i were optimized:

$$G^E = y_{3+}y_{4+}L_{3+,4+:O:Va} + y_{4+}y_{6+}L_{4+,6+:O:Va} + y_{3+}y_{6+}L_{3+,6+:O:Va} y_O y'_{Va} \quad (5)$$

The Gibbs energy model for UO_2 must be minimized in order to find the fractions of ionic constituents which give the lowest Gibbs energy for each composition.

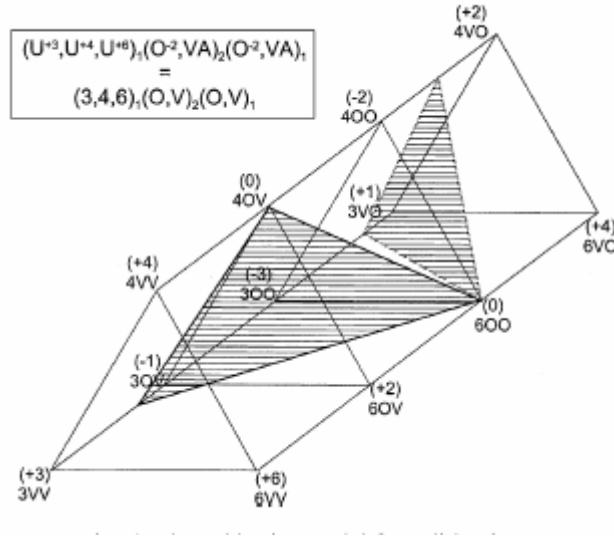
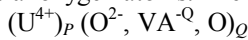


Figure 1. The sublattice model for solid $UO_{2\pm x}$

3.4 Liquid Phase

The ionic two-sublattice model^[2,3] was adopted for the description of the liquid, with one sublattice for cations and one for anions, hypothetical vacancies with an induced charge and neutral oxygen atoms. The model is:



where $y_{O^{2-}}$, y_{Va} and y_O denote the site fractions of divalent oxygen ions, vacancies and neutral oxygens on the second sublattice. P and Q are equal to the average charge of the opposite sublattice:

$$P = Qy_{Va} + 2y_{O^{2-}}$$

$$Q = 4$$

(6)

The induced charge of the vacancies corresponds to the average charge of the cation sublattice: $Q = 4$. P varies via the site fractions $y_{O^{2-}}$ and y_{Va} with the composition in order to keep the phase electrically neutral. The Gibbs energy of the liquid phase is given by the following expression:

$$\begin{aligned}
 G^{\text{Liquid}} = & y_{\text{O}^{2-}} {}^0G_{\text{U}^{4+};\text{O}^{2-}} + y_{\text{Va}} {}^0G_{\text{U}^{5+};\text{Va}} + y_{\text{O}} {}^0G_{\text{O}} \\
 & + \text{QRT}(y_{\text{O}^{2-}} \ln y_{\text{O}^{2-}} + y_{\text{Va}} \ln y_{\text{Va}} + y_{\text{O}} \ln y_{\text{O}}) \\
 & + y_{\text{O}^{2-}} y_{\text{Va}} ({}^0L_{\text{U}^{5+};\text{O}^{2-};\text{Va}}) + (y_{\text{O}^{2-}} - y_{\text{Va}}) ({}^1L_{\text{U}^{4+};\text{O}^{2-};\text{Va}}) + (y_{\text{O}^{2-}} - y_{\text{Va}})^2 ({}^2L_{\text{U}^{5+};\text{O}^{2-};\text{Va}}) \quad (7) \\
 & + y_{\text{O}^{2-}} y_{\text{O}} {}^0L_{\text{U}^{4+};\text{O}^{2-};\text{O}}
 \end{aligned}$$

${}^0G_{\text{U}^{4+};\text{O}^{2-}}$, ${}^0G_{\text{U}^{5+};\text{Va}}$, and ${}^0G_{\text{O}}$ are the reference terms, corresponding to the Gibbs energy of respectively pure UO_2 , uranium and fictitious oxygen liquid phases. ${}^0L_{\text{U}^{4+};\text{O}^{2-};\text{Va}}$, ${}^1L_{\text{U}^{4+};\text{O}^{2-};\text{Va}}$, and ${}^2L_{\text{U}^{4+};\text{O}^{2-};\text{Va}}$ are the interaction parameters describing the liquid phase in the U– UO_2 composition range. ${}^0L_{\text{U}^{4+};\text{O}^{2-};\text{O}}$ is added to describe the oxygen enriched liquid.

3.5 Gas phase

The gas phase is described as an ideal mixture containing the gaseous species U, O, O_2 , O_3 , O_1U_1 , O_2U_1 and O_3U_1 . The Gibbs energy of the gas phase is given as

$$G^{\text{g}} = \sum_i y_i {}^0G_i^{\text{g}} + RT \sum_i y_i \ln y_i + RT \ln P/P_0 \quad (8)$$

where y_i is the mole fraction of the species i in the gas phase. ${}^0G_i^{\text{g}}$ represents the standard Gibbs energy of species i of the gas phase. R is the gas constant, and P_0 the standard pressure.

IV. RESULTS AND DISCUSSIONS

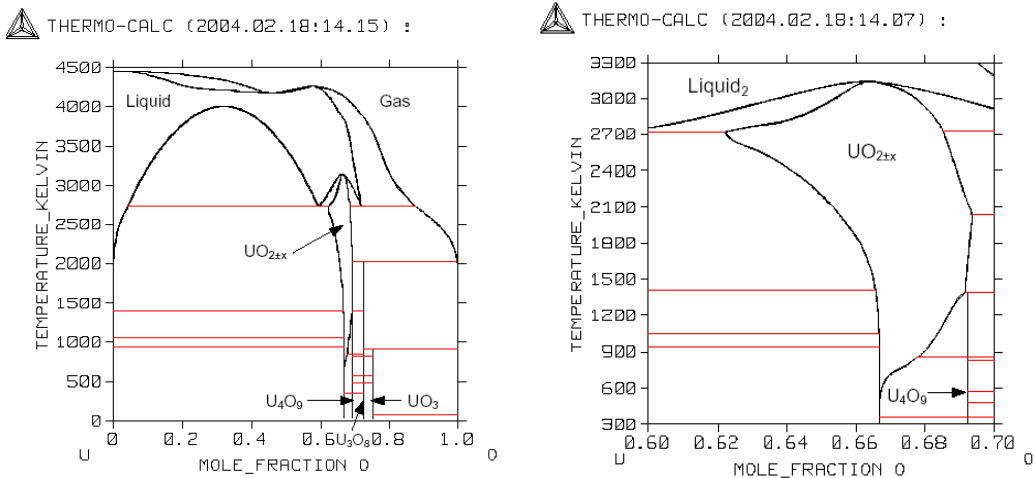


Figure 2. Calculated phase diagram for U-O system

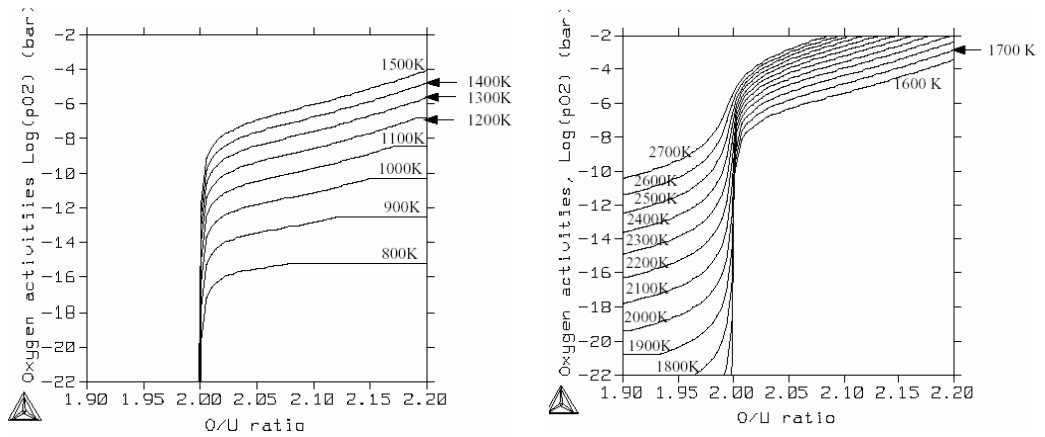


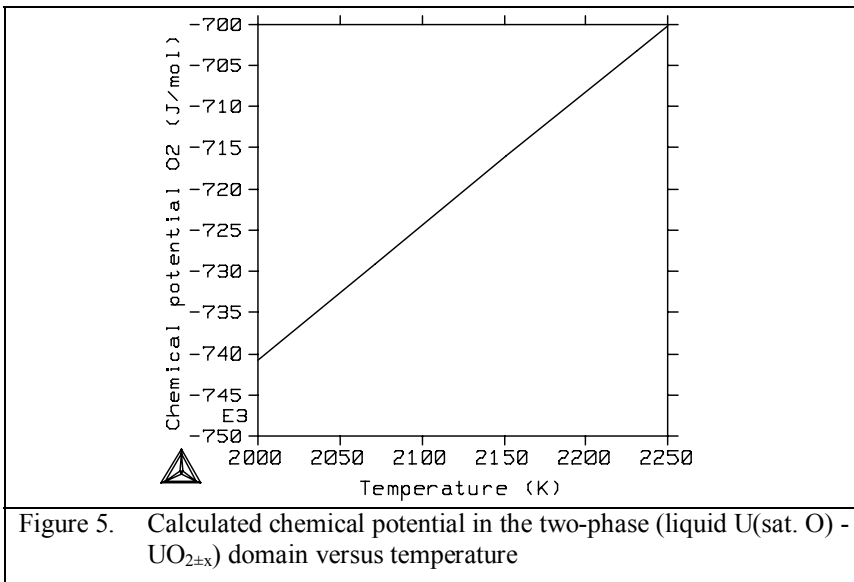
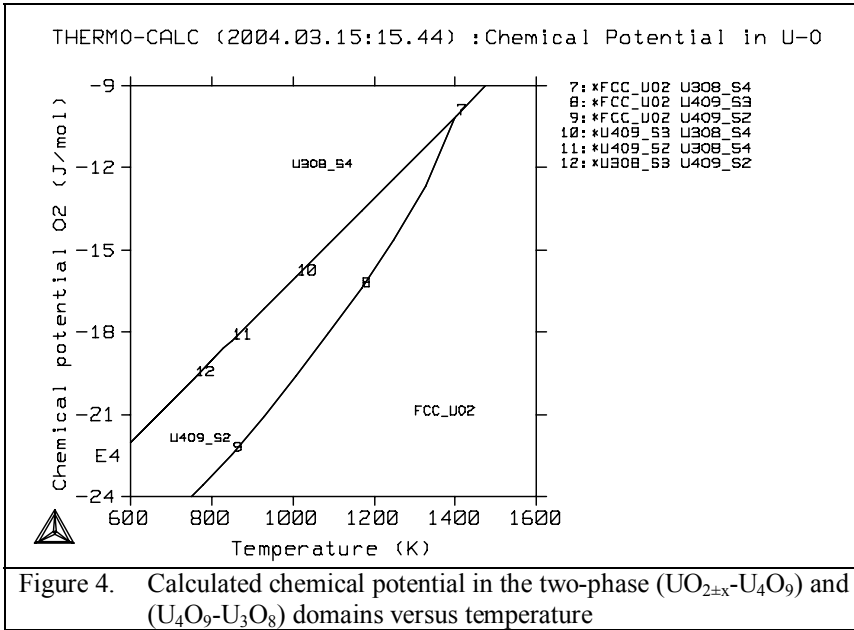
Figure 3. Oxygen activities in UO_{2+x} at temperature range of 800-2700 K

The calculated phase diagram of the U–O system at 1 bar is shown in Figure 2, while the calculated and experimental^[3,12] standard enthalpy, entropy and heat capacity of the stoichiometric oxides at 298.15 K are presented in Table 1. It is obvious that the properties of the stoichiometric oxides are in good agreement with the reported experimental data. In Figure 3, the calculated oxygen partial pressure in the single phase UO_{2+x} is given for the temperature of 800 up to 2700 K. The agreement with the experimental data is also very satisfactory for the whole composition and temperature range. It can be said here, that the three-sublattice model used to describe the properties of the uranium dioxide reproduces well the variation of the oxygen potential.

The major defects in UO_{2-x} are the oxygen vacancies in connection with a charge transfer in the cation sublattice, leading to the presence of U^{3+} cations. The fraction of U^{3+} decreases with oxygen concentration. In the UO_{2+x} composition range, the major defects are interstitial oxygen anions in connection with the presence of U^{6+} in the cation sublattice. The calculated chemical potential in the two phase UO_{2+x} - U_4O_9 , and U_4O_9 - U_3O_8 as well as liquid U- UO_{2-x} domains are shown in Figure 4 and 5. The calculated values indicate a good agreement with the selected experimental. The calculated oxygen partial pressures in all two-phase regions of the phase diagram are presented in Figure 6.

Table 1. Calculated and experimental^[3,12] standard enthalpy, entropy and heat capacity of the stoichiometric oxides at 298.15 K.

Oxide	$\Delta H_f^{\circ}(298.25\text{K})$ (J/mol atom)		$S^{\circ}(298.15\text{K})$ (J/mol atom K)		$C_p^{\circ}(298.15\text{K})$ (J/mol atom K)	
	Calculation	Experiment	Calculation	Experiment	Calculation	Experiment
UO_2 (s)	-361 374	-361 667 \pm 333	25.65	25.68 \pm 0.07	20.98	21.2 \pm 0.03
U_4O_9 (s)	-346 864	-347 077 \pm 523	25.73	25.70 \pm 0.5	22.35	22.57 \pm 0.05
U_3O_8 (s)	-325 220	-324 979 \pm 218	25.83	25.68 \pm 0.05	21.73	21.63 \pm 0.04
UO_3 (s)	-305 950	-304 375 \pm 750	24.03	24.92 \pm 0.33	20.42	20.46 \pm 0.07
U (g)	+534 996	+533 000 \pm 8000	199.8	199.8 \pm 0.1	23.69	23.69 \pm 0.04
UO (g)	+7 954	+15 250 \pm 8500	126.1	124.4 \pm 1.0	19.67	21 \pm 1.0
UO_2 (g)	-158 176	-159 267 \pm 6667	88.8	88.8 \pm 1.33	19.84	19.83 \pm 0.67
UO_3 (g)	-198 613	-199 800 \pm 375	77.4	77.4 \pm 0.5	16.12	16.12 \pm 0.5



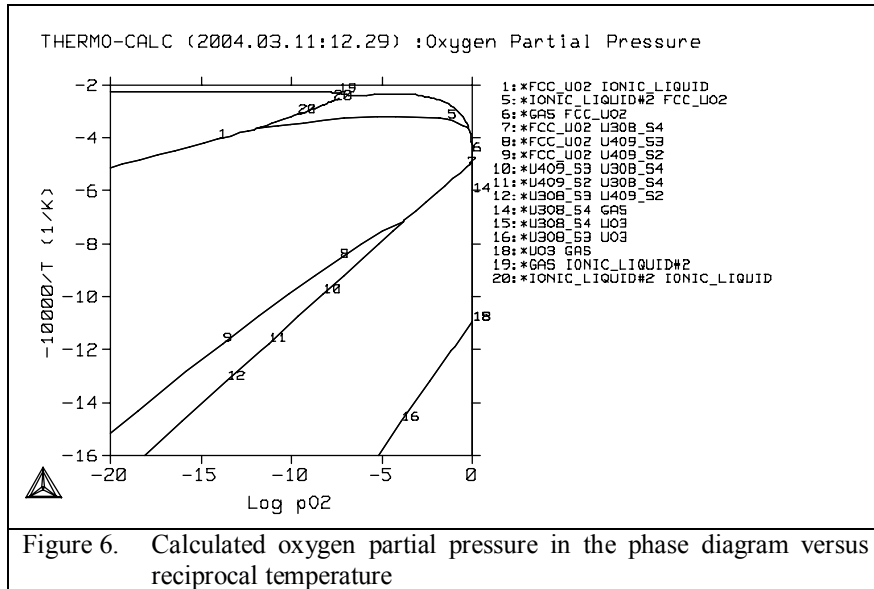


Figure 6. Calculated oxygen partial pressure in the phase diagram versus reciprocal temperature

The calculated compositions and temperatures of all invariant reactions are presented in Table 2. The calculated congruent melting point of UO_2 is equal to 3142 K for a O/U ratio of 1.98. These results are consistent with the selected experimental data of 3138 ± 23 K for the temperature. The calculated O/U ratio is a little bit too low but is still within the experimental uncertainty on the oxide composition at melting, ± 0.02 ^[6]. The calculated boiling temperature of liquid UO_2 is equal to 3842 K which is consistent with the experimental values of 3820 K from BENEZECH^[13] and of 3817 K from BREITUNG^[14]. In the present study, the boiling point of liquid UO_2 is not congruent. In fact, there are two azeotropic compositions, one maximum and one minimum (when regarding temperature) at constant pressure. This behaviour corresponds to the congruent vaporization as observed for UO_{2-x} in experiments under vacuum (or effusion) conditions^[15-17]. This tendency goes on at high temperature for the equilibrium between liquid and gas^[6]. In the present assessment, the congruency liquid/gas appears for an oxygen mole fraction of 0.58 for 1 bar total pressure as shown in Figure 2. Furthermore, in the experimental investigations of the boiling point of liquid UO_2 , the congruency is supposed but the final liquid composition is never measured. At low temperature, the limit of the hyperstoichiometric composition domain of the dioxide is well reproduced as shown in Figure 2, displaying the domain of stability of the uranium dioxide. In the $(\text{U}_4\text{O}_9\text{-UO}_{2+x})$ two-phase field, the oxygen solubility limit remains relatively flat until 800-900 K. This can be related to a tendency to the demixing of UO_2 , which is consistent with the oxygen activity curves in Figure 3. Moreover, experimental investigations show that the U_4O_9 structure can be described as an arrangement of cuboctahedric oxygen defects in a fluorite crystal with a parameter equal to four times the one of UO_2 and a composition of $\text{UO}_{2.23}$ (compared to $\text{UO}_{2.25}$)^[18]. In this way, U_4O_9 could be modeled as the same phase as UO_2 that would demix for a limiting oxygen content. This could explain both phase diagram and thermodynamics at low temperature in this composition range. It shows that the U_4O_9 phase is complex and requires other investigations to better understand this domain of the phase diagram.

Table 2. Calculated temperatures and oxygen compositions for all invariant reactions

T (K)	Invariant transformation (mole fraction O)
4252	Liquid (0.58) = Gas (0.58)
4182	Liquid (0.46) = Gas (0.46)
3142	UO ₂ (0.664) = Liquid (0.664)
2727	Liquid (0.719) = UO _{2+x} (0.685) + Gas (0.875)
2719	Liquid 2 (0.594) = Liquid 1 (0.040) + UO _{2-x} (0.628)
2032	U ₃ O ₈ -S4 (0.727) = UO _{2+x} (0.693) + UO _{2-x} (0.628)
1408	Liquid (2 × 10 ⁻⁷) = U-bcc (0) + UO _{2-x} (0.665)
1399	U ₄ O ₉ -S3 (0.692) = UO _{2+x} (0.691) + U ₃ O ₈ -S4 (0.727)
1049	U-bcc (0) = U-tetragonal (0) + UO _{2-x} (0.666)
942	U-tetragonal (0) = U-orthorhombic (0) + UO _{2-x} (0.667)
913	UO ₃ (0.75) = U ₃ O ₈ -S4 (0.727) + Gas (1.0)
850	U ₄ O ₉ -S3 (0.692) = U ₄ O ₉ -S2 (0.692)
830	U ₃ O ₈ -S4 (0.727) = U ₃ O ₈ -S3 (0.727)
598	UO ₃ (0.75) = U ₃ O ₈ -S (0.727) + Gas (1.0)
568	U ₃ O ₈ -S3 (0.727) = U ₃ O ₈ -S2 (0.727)
483	U ₃ O ₈ -S2 (0.727) = U ₃ O ₈ -S (0.727)
348	U ₄ O ₉ -S2 (0.692) = U ₄ O ₉ -S (0.692)
1878	U ₃ O ₈ -S4 decomposition in air
861	UO ₃ decomposition in air

V. CONCLUSION

In this present work, a set of thermodynamic modeling of the very complex U-O binary system has been presented, based on the critical assessment of the very numerous experimental information, concerning both phase diagram and thermodynamic properties.

A set of consistent model parameters was obtained that describes successfully both the phase diagram and the oxygen chemical potential data in the whole composition range. It shows that the three-sublattice model is suitable to describe complex oxides such as UO_{2±x}.

It is shown that the consistency between the calculated results and the experimental data is quite satisfactory.

VI. RECOMMENDATION

To continue this work, the homogeneity ranges of the U₄O_{9-y} and U₃O_{8-y} compounds will be represented in the future assessment.

Concerning the experimental data critical review, there still remain some inconsistencies on the thermodynamic data of the gas species UO, UO₂ and UO₃ (enthalpy, entropy, heat capacity and partial pressure). In the next assessment, these gas properties are to be fixed on the basis of a critical review in order to improve the description of the congruent equilibria between the condensed and gas phases

VII. REFERENCES

1. CHEVALIER, P.Y., and FISCHER, E., "Thermodynamic Modeling of the O-U-Zr System", J. Nuclear Materials, Vol. 257, 1998, p.213.

2. SUNDMAN, B., and ÅGREN, J., "A Regular Solution Model for Phases with several Components and Sublattices, suitable for Computer Applications", *J. Phys. Chem. Solids* 42, 1981, p.297.
3. SUNDMAN, B., JANSSON, B., and ANDERSSON, J.O., "The Thermo-Calc Databank System", *Calphad* 9, 1985, p.153.
4. SUNDMAN, B., JANSSON, B., and SHALIN, M., "Thermodynamic Calculations Made Easy", *J. Phase Equil.*, 1993, pp.557-562.
5. LABROCHE, D., PhD Thesis, INPG Grenoble, 2000.
6. BAICHI, M., PhD Thesis, INPG Grenoble, 2001.
7. GUÉNEAU C. et al, *Journal of Nuclear Materials*, Vol. 304, 2002, pp.161-175.
8. DINSDALE, A.T., "SGTE Data for Pure Elements", *Calphad* 15 (4), 1991, p.317. (Updated in SGTE Database)
9. ANSARA, I., and SUNDMAN, B., Scientific Group Thermodata Europe, in: Glaser P.S., (Ed.), *Computer Handling and Determination of Data*, North Holland, Amsterdam, 1986, p.154.
10. MAC INNES, D.A., and CATLOW, C.R.A., *J. Nuclear Materials*, Vol. 89, 1980, p.354.
11. WILLIS, B.T.M., *Nature*, Vol. 197, London, 1963, p.755.
12. GREUTE, I., FURGER, J., KONINGS, R.J.M., LEMIRE, R.J., MULLER, A.B., NGUYEN-TRUNG, C., and WARNER, H., "Chemical Thermodynamic 1 – Chemical Thermodynamic of Uranium", edited by WARNER, H., and FOREST, I., OECD, North Holland, Amsterdam, 1992, p.30.
13. BENEZECH, G., COUTURES, J.P., and M. FOEX, M., *Thermodynamic Nuclear Materials Proceeding 4th Symposium, Vienna 1974, 1975*, p.337.
14. BREITUNG, W., and REIL, K.O., U.S. Nuclear Regulations Commission, Report NUREG-CR-4295, 1985, p.1.
15. PATTORET, A., PhD thesis, Universite Libre de Bruxelles, 1969.
16. ACKERMANN, R.J., RAUH, E.G., and CHANDRASEKHARAI AH, M.S., *J. Phys. Chem.*, Vol. 73, 196, p.762.
17. EDWARDS, R.K., CHANDRASEKHARAI AH, M.S., and DANIELSON, P.M., *High Temp. Sci.* 1, 1969, p.98.
18. BEVAN, D.J.M., GREY, I.E., and WILLIS, B.T.M., *J. Solid. State Chem.*, Vol. 61, 1986, p.1.